

# High resolution imaging with impulse based thermoacoustic tomography

Stephan Kellnberger, Amir Hajiaboli, George Sergiadis, Daniel Razansky and Vasilis Ntziachristos

Institute for Biological and Medical Imaging (IBMI),  
Technische Universität München and Helmholtz Zentrum München,  
Ingolstaedter Landstrasse 1, D-85764 Neuherberg, Germany

## ABSTRACT

Existing imaging modalities like microwave- or radiofrequency (RF) induced thermoacoustic tomography systems show the potential for resolving structures deep inside tissue due to the high penetration properties of RF. However, one of the major drawbacks of existing thermoacoustic tomography systems with pulse modulated carrier frequency excitation is the compromise between efficient signal generation and attainable spatial resolution. In order to overcome limitations of conventional thermoacoustic imaging methods, we herein present and experimentally validate our novel approach towards high resolution thermoacoustic tomography. Instead of carrier-frequency amplification, we utilize ultrahigh-energy electromagnetic impulses at nanosecond duration with near-field energy coupling, thus maintaining thermoacoustic signal strength without compromising spatial resolution. Preliminary experiments on highly absorbing objects, consisting of copper wires with characteristic sizes of  $\sim 100 \mu\text{m}$ , reveal the resolution performance which yields  $160 \mu\text{m}$ . Furthermore, benefits like its cost effectiveness, simplicity and compactness with the potential application in small animal imaging as well as human body imaging show that thermoacoustic tomography with impulse excitation is a promising imaging modality which has a broad range of applications.

**Keywords:** thermoacoustic tomography, photoacoustic imaging, biological imaging, near-field imaging, electromagnetic impulses

## 1. INTRODUCTION

Thermoacoustic tomography (TAT) is an imaging modality which combines both the advantages of ultrasound imaging with its high resolution and of microwave imaging with its good contrast. Being firstly described by Alexander Graham Bell,<sup>1</sup> the thermoacoustic effect corresponds to absorption of pulsed electromagnetic (EM) energy in biological tissue with subsequent emanation of acoustic pressure waves according to thermoelastic expansion of tissue.<sup>5</sup> After irradiation of lossy tissue with EM pulses in the microwave or RF region, the dissipated transient energy is transformed into kinetic energy, causing a subsequent heating of the object.<sup>6</sup> Tomography is yielded through acquisition of thermoacoustic signals with an ultrasonic detector at distinct projections around the object followed by the mathematical inversion of the signals. The reconstructed image illustrates areas and points of electromagnetic power deposition in the imaged object.<sup>4</sup>

Whereas in its light based counterpart optoacoustic tomography (OAT) contrast is yielded by optical absorption of tissue, thermoacoustic tomography maps different dielectric properties of biological tissue like low conducting fat tissue ( $\sigma = 0.015 \text{ S m}^{-1}$  at 10 MHz) versus high conductive muscle tissue ( $\sigma = 0.8 \text{ S m}^{-1}$  at 10 MHz).<sup>9</sup> In addition, cancerous breast tissue provides more than double the absorption of environing healthy tissue,<sup>6</sup> making TAT a promising candidate for breast cancer imaging.<sup>12</sup>

Although optoacoustics offers higher and more applicable intrinsic contrast in biological tissue, contrast in thermoacoustics can be enhanced by extrinsically-administered agents like carbon nanotubes.<sup>7</sup> Furthermore, with biological tissue penetration depths of  $\sim 25\text{cm}$  at 10 MHz<sup>6, 9</sup>, thermoacoustic tomography has potential for broader clinical dissemination compared to optoacoustics.

Although thermoacoustic tomography has promising benefits, certain drawbacks in terms of resolution and signal to noise ratio restrained thermoacoustic tomography from becoming a widely used imaging modality.

One important parameter in thermoacoustic tomography is the achieved resolution. Since the spatial resolution directly relates to the duration of the excitation pulse, high resolution images demand ultrashort pulses in the nanosecond range.<sup>8, 10</sup>

Consequently, the shorter the excitation pulse the less energy one pulse contains. Conventional thermoacoustic tomography systems which are based on narrowband pulse modulated microwave radiation<sup>4, 6</sup>, therefore prolonged the excitation pulse to hundreds of  $\mu\text{s}$ <sup>6, 10</sup>, increasing energy per pulse on the one hand but also mitigating high resolution requirements.

In order to overcome characteristic disadvantages related to conventional thermoacoustic tomography, we propose a novel approach which is the model of high energy ultrawideband excitation. Instead of amplifying modulated carrier frequency pulses, we are generating high energy ultrashort pulses in the range of tens of nanoseconds. By these means, we maintain high resolution due to the short pulse width as well as good SNR since our sample is placed in the vicinity of the energy coupling element which deposits energy in the object.<sup>2, 3</sup>

In this paper, we present preliminary results of our impulse-based thermoacoustic tomography approach. High resolution images of absorbing wires with a spatial resolution of  $160\ \mu\text{m}$  were attained, with the resolution being mainly limited by the detection bandwidth of the ultrasonic transducers.

## 2. MATERIALS AND METHODS

### 2. 1. Experimental setup

A simplified scheme of our thermoacoustic tomography setup is depicted in figure 1.<sup>8</sup> A custom made impulse generator produces high-voltage pulses with peak amplitudes of up to 30 kV and energies ranging from hundreds of mJoules to Joules. The time duration of the electromagnetic impulse lies in tens of nanoseconds, creating a broadband excitation of the sample. The impulse generator is triggered by a function generator (Model 33210A Function/Arbitrary Waveform Generator, Agilent Technologies, Santa Clara, CA, USA) and is set to a repetition frequency of 10 Hz. An energy coupling element, shielded with a high voltage isolating shrinking tube (Model HSR3000, 350 kV  $\text{cm}^{-1}$ , 3M, St. Paul, MN, USA) is connected to the output of the impulse generator unit and couples electromagnetic energy to the sample which is placed in close vicinity. The object is rotated with a rotational stage (Model PR50PP, Newport Corporation, Irvine, CA, USA) and data is acquired in  $2^\circ$  steps in-plane over  $360^\circ$ , resulting in 180 projections. A second linear stage (LTA-HS, Newport Corporation, Irvine, CA, USA) translates the object in vertical position to achieve volumetric imaging of the object. Thermoacoustically induced signals were detected with a cylindrically focused ultrasonic transducer with central frequency at 7.5 MHz and 77.5% bandwidth (focal distance 25.4 mm, Model V320, Olympus-NDT, Waltham, MA, USA). Acquired signals were recorded at a sample rate of 200MSps with a resolution of 8 bit by a digital phosphor oscilloscope (Model DPO7254, Tektronix Inc., Beaverton, OR, USA) and averaged 20 times at each projection position. Additionally, we added a 300 kHz hardware high pass filter in the detection path to reduce saturation effects on the detector, caused by stray coupling from the high voltage impulses. All devices were controlled with a personal computer (PC) and a custom-developed LabVIEW programme (LabVIEW2009, National Instruments, Austin, TX, USA). Finally, all images were reconstructed with a circular back-projection algorithm.<sup>8</sup>

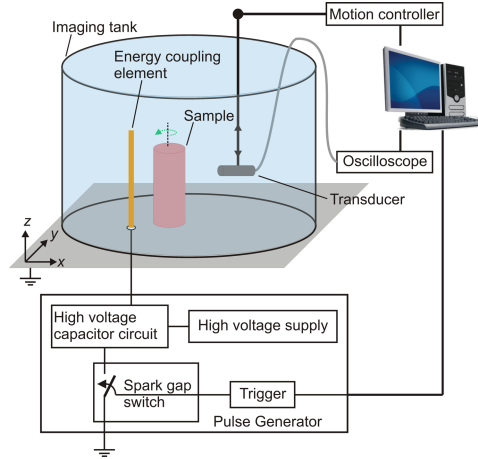


Figure 1. Schematic diagram of the high resolution thermoacoustic tomography setup with a schematic of the pulse generator

## 2. 2. Contrast mechanism and spatial resolution

According to the thermoacoustic wave equation, thermoacoustic pressure waves which are induced by local absorption of electromagnetic energy can be described by

$$\nabla^2 p(\vec{r}, t) - \frac{1}{v_s^2} \frac{\partial^2 p(\vec{r}, t)}{\partial t^2} = -\rho_m \beta \frac{\partial^2 T(\vec{r}, t)}{\partial t^2} = -\frac{\beta}{C} \frac{\partial H(\vec{r}, t)}{\partial t} \quad (1)$$

with pressure  $p(\vec{r}, t)$ , heating function  $H(\vec{r}, t)$ , local temperature rise  $T(\vec{r}, t)$ , speed of sound  $v_s$ , mass density  $\rho_m$ , specific heat capacity  $C$  and thermal expansion coefficient  $\beta$ .

As mentioned before, contrast in thermoacoustic tomography is given by the differences of dielectric properties of the tissue under test, according to the formula

$$H(\vec{r}) = \int_V \frac{\sigma}{2} |\vec{E}|^2 dV + \int_V \frac{\epsilon_0 \epsilon_r''}{2} |\vec{E}|^2 dV + \int_V \frac{\mu_0 \mu_r}{2} |\vec{H}_{mag}|^2 dV = P_{cond} + P_{el} + P_{mag} \quad (2)$$

with conductivity losses  $P_{cond}$ , dielectric losses  $P_{el}$  and magnetic losses  $P_{mag}$ . Disregarding magnetic losses, the main contrast can be achieved by regions in tissue with high electric losses. Therefore, thermoacoustic images are equivalent maps of conductivity distributions in the sampled object.

According to<sup>11</sup>, the spatial resolution can be determined with the equation

$$R \approx 0.92 \frac{v_s}{f_c} = 0.92 \lambda_c \quad (3)$$

with the wavelength  $\lambda_c$  at the cut-off frequency of the bandwidth and the speed of sound  $v_s$ . To determine the spatial resolution of our tomography system, we imaged two highly absorbing copper wires with diameter of  $\sim 100 \mu\text{m}$  and calculated the full width half maximum (FWHM) of the reconstructed image.

## 3. RESULTS

In order to assess the resolution of our thermoacoustic system, we imaged two absorbers made of copper wire with a characteristic diameter of  $\sim 100 \mu\text{m}$ . The results are depicted in figure 2. In the reconstruction in figure 2(a) the two wires can be clearly detected. Figure 2(b) depicts a one-dimensional profile through one wire of the reconstructed image, showing a full width half maximum of  $160 \mu\text{m}$ . Taking into account the available detection bandwidth of the ultrasonic transducer (77% bandwidth at a central frequency of 7.5MHz), the attainable resolution is mainly limited by the ultrasonic transducer bandwidth and can be further improved by transducers with larger detection bandwidth.

In addition, figure 2(c) shows the measured signal of one projection, representing the two distinct signals coming from the two copper wires.

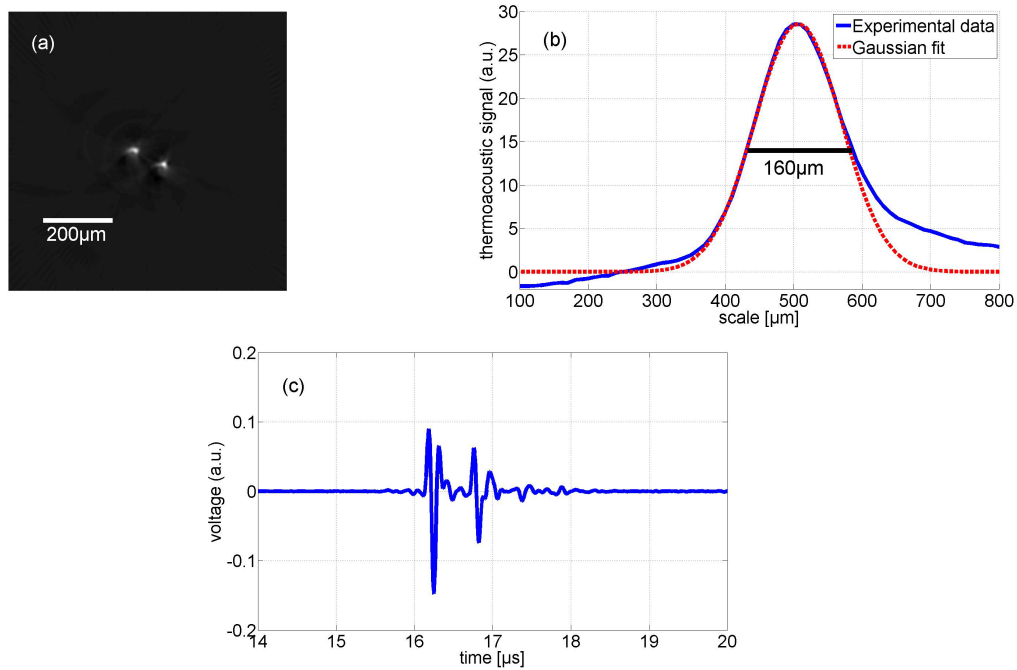


Figure 2. Thermoacoustic resolution study. (a) Thermoacoustic image of two copper wires with sizes of 160  $\mu\text{m}$ ; (b) One-dimensional cut through one absorbing element of figure 2(a) for validation of in-plane resolution with corresponding Gaussian fit; (c) Example of thermoacoustic response measured with a 7.5 MHz transducer

#### 4. CONCLUSIONS

In this work, we presented a new approach towards thermoacoustic tomography. By utilizing ultrahigh energy nanosecond electromagnetic impulses instead of narrowband modulated pulses, we maintained high resolution without compromising signal to noise ratio. In a resolution study we imaged two highly absorbing copper wires with dimensions of 100  $\mu\text{m}$ .

After reconstruction, the two wires can clearly be identified. Calculating the full width half maximum of one wire reveals the superior resolution which goes down to 160  $\mu\text{m}$ , being mainly limited by the detection bandwidth of the ultrasonic transducer.

Thus, we believe that our near-field radiofrequency thermoacoustic tomography system with its high resolution, cost-effectiveness, simplicity and high penetration depth is a powerful tool with versatile applications in small animal as well as clinical imaging. Future work includes the administration of conductive contrast agents to enhance thermoacoustic signals and to perform molecular imaging for targeted imaging applications.

## REFERENCES

- [1] Bell, A. G., "On the production and reproduction of sound by light" *Am. J. Sci.* **20**, 305-24 (1880).
- [2] Bowen, T., "Radiation induced thermoacoustic soft tissue imaging" *Proc. IEEE Ultrasonics Symp.* **2**:817-22 (1981).
- [3] Bowen, T., Nasoni, R. L., Pifer, A. E. and Sembroski, G. H., "Some experimental results on the thermoacoustic imaging of soft tissue-equivalent phantoms" *Proc. IEEE Ultrasonics Symp.* **2**:823-27 (1981).
- [4] Kruger, R. A., Kiser, W. L., Miller, K. D. and Reynolds, H. E., "Thermoacoustic CT: Imaging principles" *Proc. SPIE*, Vol. **3916**, 150 (2000).
- [5] Kruger, R. A., Kopecky, K. K., Aisen, A. M., Reinecke, D. R., Kruger, G. A. and Kiser, W. L., "Thermoacoustic CT with radio waves: A medical imaging paradigm" *Radiology* **211**, 275-78 (1999).
- [6] Ku, G. and Wang L.-H., "Scanning thermoacoustic tomography in biological tissue" *Med. Phys.* **27**(5): 1195-1202 (2000).
- [7] Pramanik, M., Swierczewska, M., Green, D. Sitharaman, B. and Wang, L.-H., "Single-walled carbon nanotubes as a multimodal-thermoacoustic and photoacoustic-contrast agent," *J. Biomed. Opt.* **14**, 034018 (2009).
- [8] Razansky, D., Kellnberger, S. and Ntziachristos, V., "Near-field radiofrequency thermoacoustic tomography with impulse excitation" *Med. Phys.* **37**(9): 4602-07 (2010).
- [9] Gabriel, S., Lau, R. W. and Gabriel, C., "The dielectric properties of biological tissues: II. Measurements in the frequency range 10 Hz to 20 GHz" *Phys. Med. Biol.* **41** 2251-69 (1996).
- [10] Xu, M. H. and Wang, L.-H., "Photoacoustic imaging in biomedicine" *Rev. Sci. Instrum.* **77**, 041101 (2006).
- [11] Wang, L.-H., [Photoacoustic Imaging and Spectroscopy] (CRC, Boca Raton) (2009).
- [12] Kruger, R. A., Miller, K. D., Reynolds, H. E., Kiser, W. L. and Kruger, G. A., "Breast cancer *in vivo*: contrast enhancement with thermoacoustic CT at 434 MHz – feasibility study" *Radiology* **216**:279-283 (2000).